The Turbulent Microstructure of Hurricane Caroline (1975)[1]

FRANCIS J. MERCERET

National Hurricane and Experimental Laboratory, NOAA, Coral Gables, Fla. 33124

(Manuscript received 11 March 1976, in revised form 19 July 1976)

ABSTRACT

Microscale horizontal velocity fluctuation measurements in Hurricane Caroline (1975) show that except in the eye, turbulent energy dissipation does not vary systematically with wind speed or altitude. Inertial subrange-shaped spectra are found below cloud base and slightly above it. At higher altitudes, some deviation from that shape may occur. The amount of energy dissipated within the body of the storm is slightly larger than that dissipated at the surface in accord with earlier estimates by residuals. The dissipation is highly intermittent with a log-normal cumulative probability distribution.

1. Introduction

Hurricane Caroline began as a tropical disturbance that crossed the west coast of Africa on 15 August 1975. It traversed the Atlantic and Caribbean without attaining tropical storm strength, but shortly after entering the Gulf of Mexico through the Yucatan Channel on 29 August it deepened and became Tropical Storm Caroline. The storm moved just north of west and slowed to a forward speed of about 5 kt while continuing to intensify. On the same day that it was named, Caroline reached hurricane strength. NOAA Research Facilities Center (RFC) aircraft were deployed to Kelly Air Force Base in Texas with the hope of monitoring the storm on the 30th before it made landfall. The RFC aircraft, a DC-6 (NOAA 39) and a WC130B

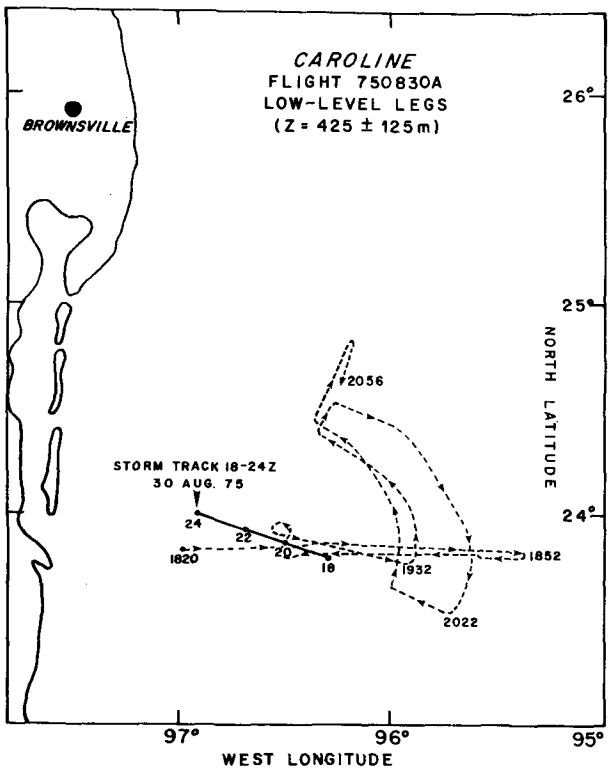

FIG. 1. Flight track below cloud base.

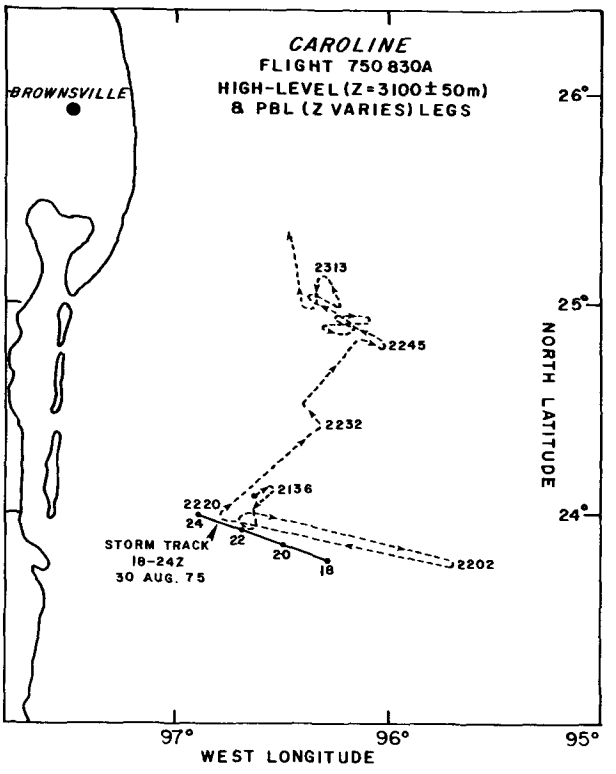

FIG. 2. High altitude and PBL flight tracks.

[1] This paper is dedicated to Brian Rice who died on 22 November 1975. Brian operated the equipment on board the aircraft during Caroline and processed much of the data on which this paper is founded. He was a valued colleague and friend.

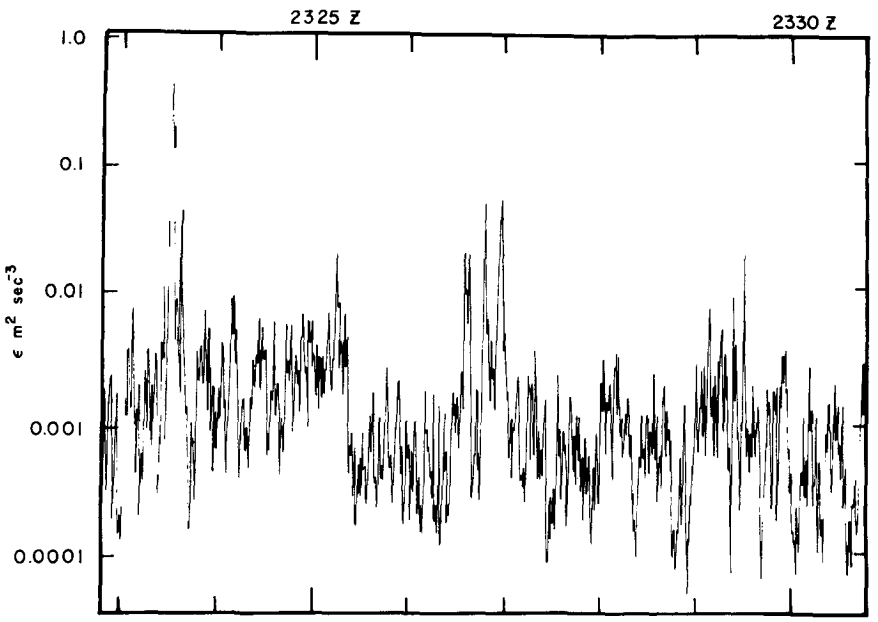

FIG. 3. Typical time series of log$_\epsilon$ (1 s smoothing).

(NOAA 41), arrived in the vicinity of Caroline around 1800 (all times GMT) on 30 August 1975 to find winds exceeding 36 m s^{-1} and a minimum sea level pressure (MSLP) of 987 mb. The storm intensified rapidly during the next 6 h and had attained a MSLP of 973 mb and a maximum recorded wind speed of 52 m s^{-1} by the time the research aircraft left the area. This paper is based on measurements made from the DC-6 between 1820 and 2335 on 30 August 1975. The flight identification number for 39C was 750830A.

Among the experiments aboard flight 750830A was a unique attempt to measure the microstructure of the turbulent velocity field in a hurricane, with primary emphasis on establishing the distribution of turbulent

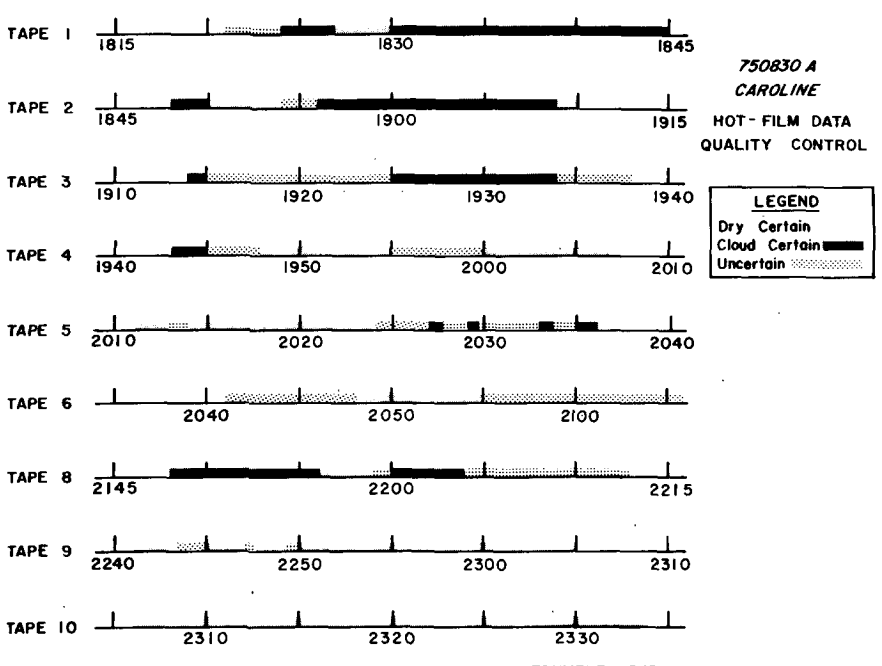

FIG. 4. Record of presence or absence of cloud touching the aircraft during data collection.

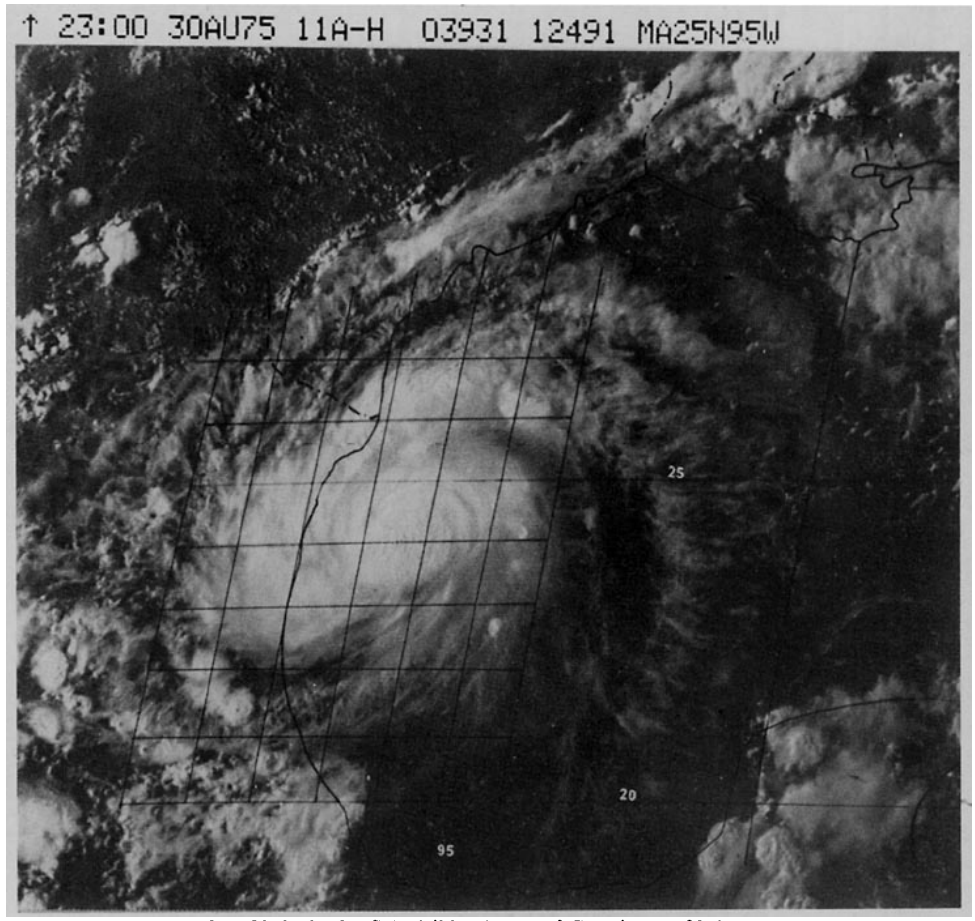

FIG. 5. 2230 GMT SMS-1 visible picture of Caroline on 30 August.

energy dissipation in a fully developed tropical storm. A Thermosystems Model 1050 hot-film anemometer[2] was installed to measure the streamwise component of the flow at scales from 50 m to 4 cm in a manner similar to that used by Merceret (1976a) in the less rigorous environment of the GATE. After data were collected over a substantial portion of the storm below cloud base (Fig. 1), the aircraft climbed to 3000 m. Descent followed in stepwise fashion between 2240 and 2330 in an attempt to fly a planetary boundary layer pattern (Fig. 2). The PBL flight pattern was too scattered to be used for a rigorous analysis of the kind exemplified by Fennell and Lemone (1974), but it contributed substantially to the clarification of the transition between the subcloud layer and the regime at 3000 m. With the exception of a period between 2056 and 2133 when the aircraft bulk data recording system failed, we obtained high-quality turbulence data synchronized with wind, temperature, humidity and liquid water data, and photography. Even during the data system outage, the turbulence data were obtained; though unsynchronized and isolated, they gave valuable information about the turbulence properties in the eye where repairs were being undertaken. Because these data are unique, it was decided to publish a descriptive summary of the results as soon as possible, with a more sophisticated analysis to follow based on the data from Caroline and on similar data from flights into Eloise and Gladys during the 1975 season. This paper presents the summary of the turbulent microstructure of Caroline.

2. Data processing

Before the signal from the anemometer was recorded, it was prewhitened to enhance the signal-to-noise ratio of playback. In the laboratory the tapes were played back into a signal processor, which recolors the information and scales it based on wind-tunnel calibrations to 1 V per meter per second in the frequency band between 2 and 2500 Hz (equivalent to a range of scales covering 50 m to 4 cm at a true airspeed of 100 m s^{-1}). Comparison of pre-flight and post-flight calibrations showed that the calibrations remained stable within 3%. The scaled velocity signal was processed in a real-time spectrum analyzer for spectra, and dissipation estimates were based on inertial subrange portions of the spectra, as described below. The dissipation esti-

[2] Mention of a proprietary product does not constitute an endorsement thereof by the author or by the National Hurricane and Experimental Meteorology Laboratory.

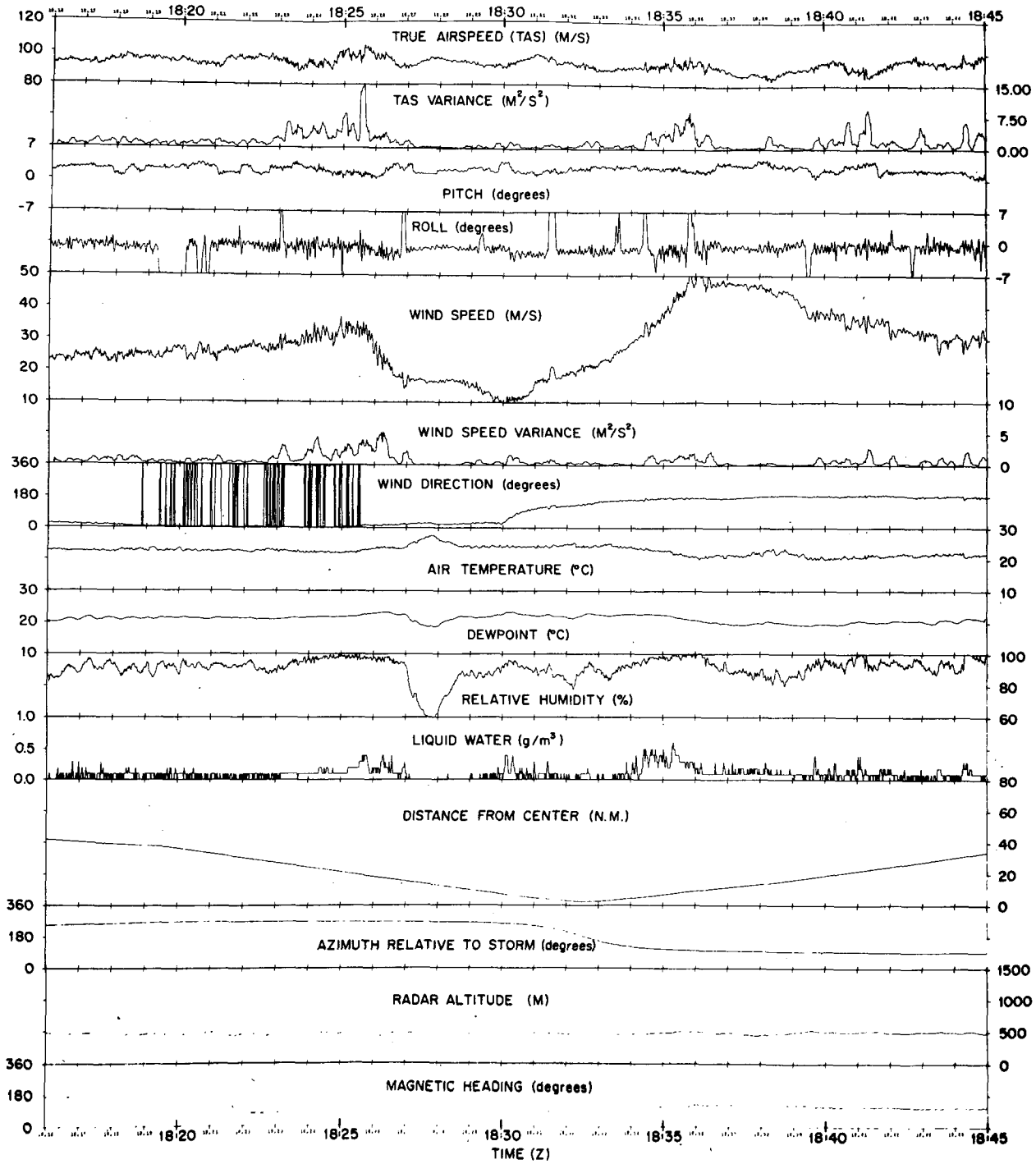

FIG. 6. Meteorological variables and aircraft parameters for turbulence tape 1.

mates (ϵ) were produced in real time as an analog signal proportional to log ϵ averaged over eight spectra each from a record of 0.125 s. The bandwidth of the analyzer was 12 Hz. The 80% confidence limit is 3 dB (Jenkins and Watts, 1968, p. 82). This signal was fed to a correlation and probability analyzer to determine its cumulative probability distribution in selected cases, and was logged on strip charts in all cases. Mean spectra were computed from the average of 512 spectra from 0.125 s records. The 99.5% confidence limit is less than 0.5 dB (*ibid.*). The base data for this paper are the time traces of log ϵ, the spectra, and the cumulative probability distributions of log ϵ. Most of the data were obtained in regions where the wind

speed was between 20 and 30 m s^{-1} though some were obtained at wind speeds as high as 45 m s^{-1} and others were obtained in the eye where wind speeds less than 10 m s^{-1} were found. We do not have enough information to be sure that the results presented here are valid in the high-energy core of the storm but the few points we have there are not inconsistent with the hypothesis that the results apply there as well.

3. The basic characteristics of the flow in the subcloud layer

As one would expect, the dissipation below 1000 m altitude is highly intermittent. Fig. 3 shows a time series of log dissipation computed from the spectral density at 648 Hz (~15 cm) (average of eight spectra) in a region of 20 m s^{-1} winds well away from the storm

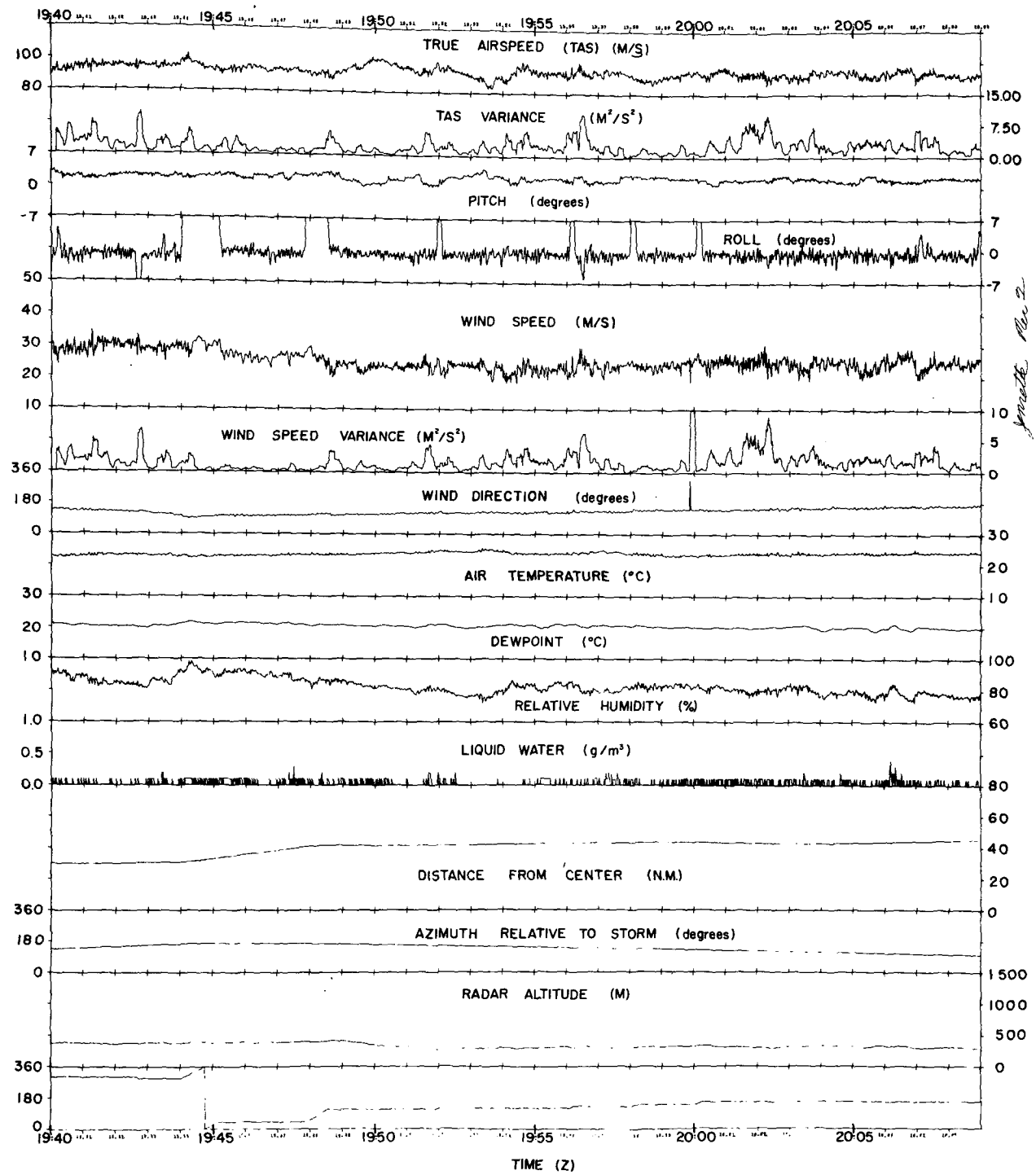

FIG. 7. As in Fig. 6 for tape 4.

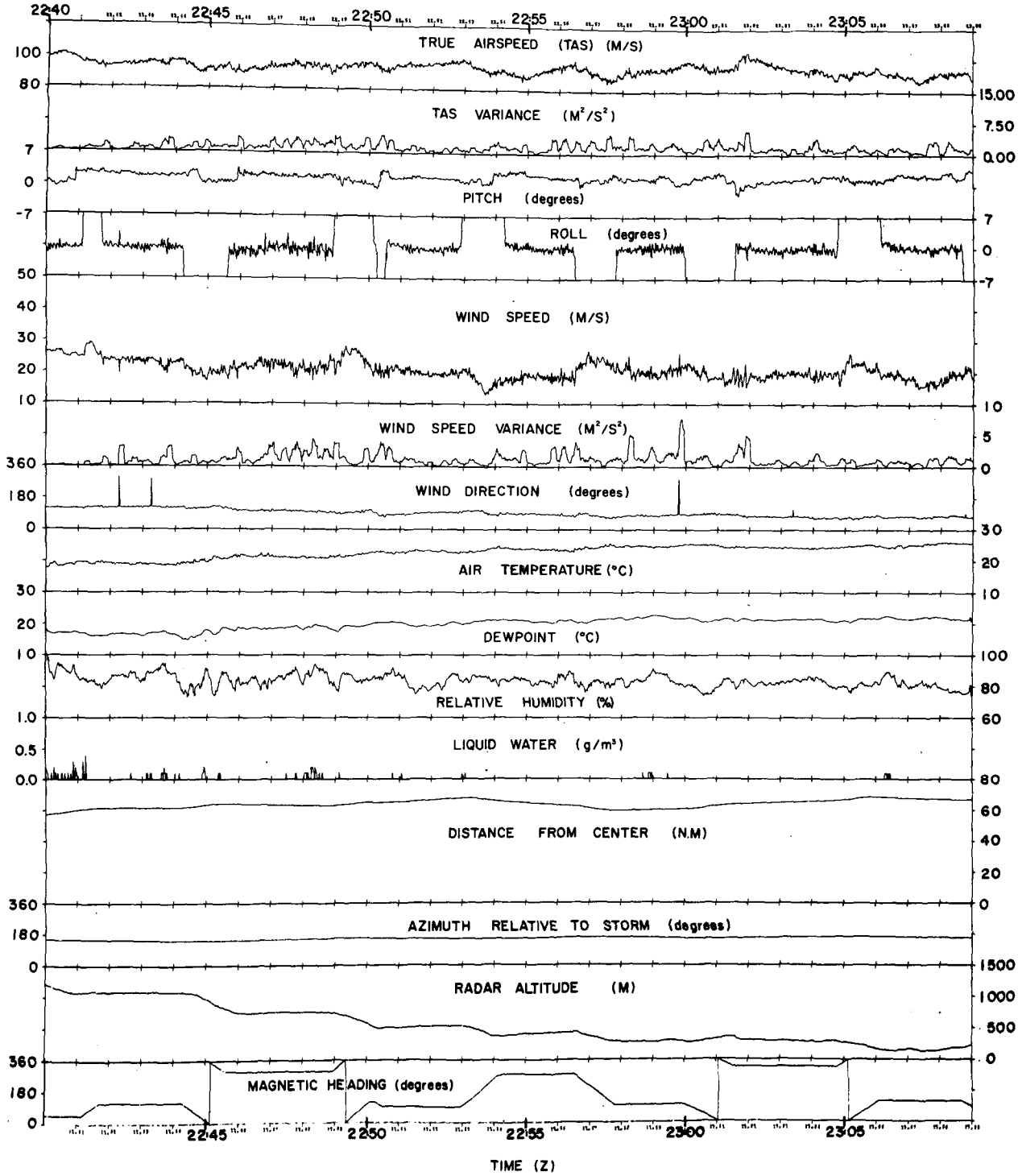

FIG. 8. As in Fig. 6 for tape 9.

center where this scale is in the inertial subrange. It typifies the fluctuations found throughout most of the storm where wind speeds exceeded 25 m s^{-1}, the fluctuations being somewhat smaller than those found in small areas of active convection. The probability distribution of the dissipation is log-normal as will be discussed below.

Below cloud base, which ranged from below 200 m to above 500 m, the spectra were inertial over a range of scales from larger than 10 m to smaller than 10 cm. That is to say, they were close to the form

$$E(f)=c_1 f^{-5/3} \tag{1}$$

throughout the range. The actual slope of the spectra

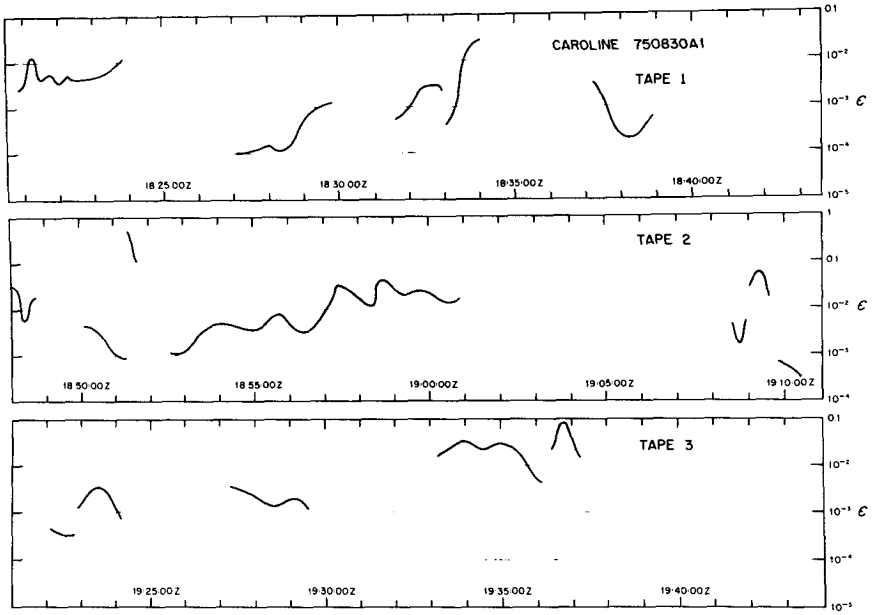

FIG. 9. Time series of logϵ (30 s manual smoothing).

averaged 1.80 ± 0.17 for a sample of 47 mean spectra each containing 512 individual spectra from 0.125 s records. The correlation coefficient for the least squares fit to (1) averaged greater than 0.99 for spectra made in the absence of cloud liquid water droplets which contaminate the signal. Dissipation rates were computed from mean spectra based on 67 s records (512 spectra) according to

$$\epsilon=\frac{2\pi}{\bar{U}}\left[\overline{2.2f^{5/3}E(f)}\right]^{\frac{3}{2}} \tag{2}$$

(where here only an overbar denotes an average over all frequencies in the sample). They varied from less than 10^{-5} m^2 s^{-3} in the eye and between active convective areas to more than 0.1 m^2 s^{-3} in a few highly active areas. The dissipation rates seemed to be locally governed and did not correlate well with position, mean wind or other bulk variables, except that the lowest value was found in the eye and the highest in heavy convection. They did correlate well with the observer's impressions of the turbulence level determined from remarks recorded on the voice track of the data tape. The higher dissipation rates were usually associated with a rough ride. Over more than 80% of the sampled area of the storm the dissipation averaged at least 3×10^{-4} m^2 s^{-3}, but not more than 3×10^{-2} m^2 s^{-3}. A "typical" value of ϵ for Hurricane Caroline might well be taken to be 3×10^{-3} m^2 s^{-3} over most of its area and 3×10^{-2} or slightly more over the balance.

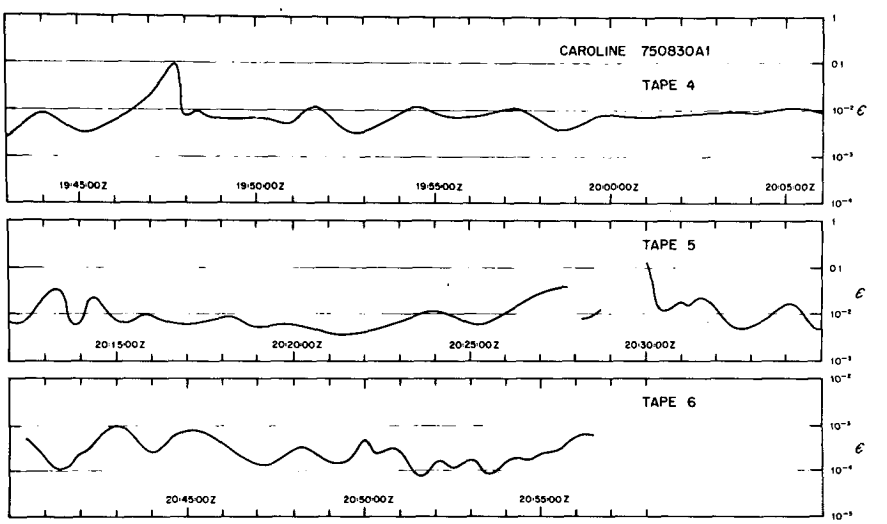

FIG. 10. As in Fig. 9 for tapes 4–6.

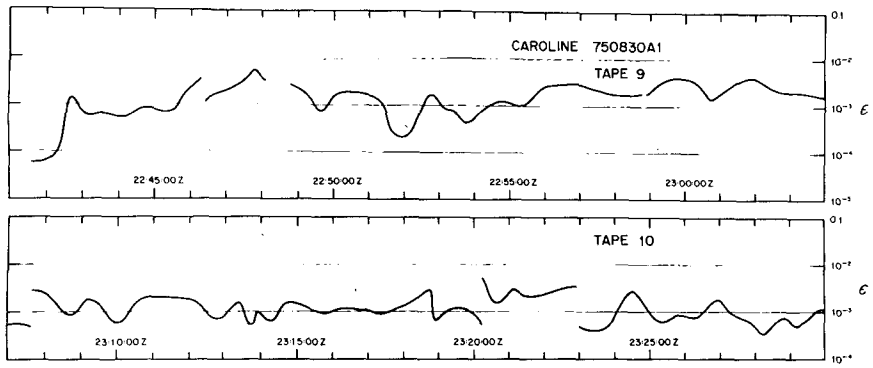

FIG. 11. As in Fig. 9 for tapes 9–10.

Note that these values are necessarily underestimates because of the stochastic nature of ϵ.

4. Details of the subcloud layer

The foregoing summary is probably at least as useful as the detailed data at this point, but summaries are often suspect, so some of the detail is included here. Anyone who wishes a more complete picture may obtain as much information as is required from the National Hurricane and Experimental Meteorology Laboratory. Fig. 4 shows the times for which data were obtained and gives an indication of their quality. Clear air data are of excellent reliability; data taken in-cloud are usually unreliable. In questionable areas the data are of uncertain quality. Reference to the flight tracks in Figs. 1 and 2, and to the SMS-1 photograph in Fig. 5, should enable the reader to place any point of interest relative to the storm, if allowance for the storm's forward motion is made. The features of the storm are evolving so that except near the time of the photograph, the flight track cannot be used with the photograph to position the aircraft relative to any specific features of the storm but the eye. Fig. 6 shows the values of bulk variables and flight parameters along a typical west-to-east radial pass through the storm at low level including penetration of the eye. Fig. 7 shows a leg in the northeast quadrant at constant distance from the center roughly parallel to a rainband. Fig. 8 shows most of the PBL flight track. These figures show the kinds of environments sampled through most of the flight. Data were also obtained at 3000 m, but only from 2145 to 2214. Validated traces of ϵ based on 1 s running averages manually smoothed over roughly $\frac{1}{2}$ min are presented in Figs. 9–11. Remember that the traces at greater resolution look like that shown in Fig. 3.

Figs. 12 and 13 show respectively the mean wind speed and ϵ as functions of distance (R) from the storm center. Similar figures can be generated for any of the variables in Figs. 6–11 if the flight track is used to determine R for each time for which the value of a variable is to be plotted.

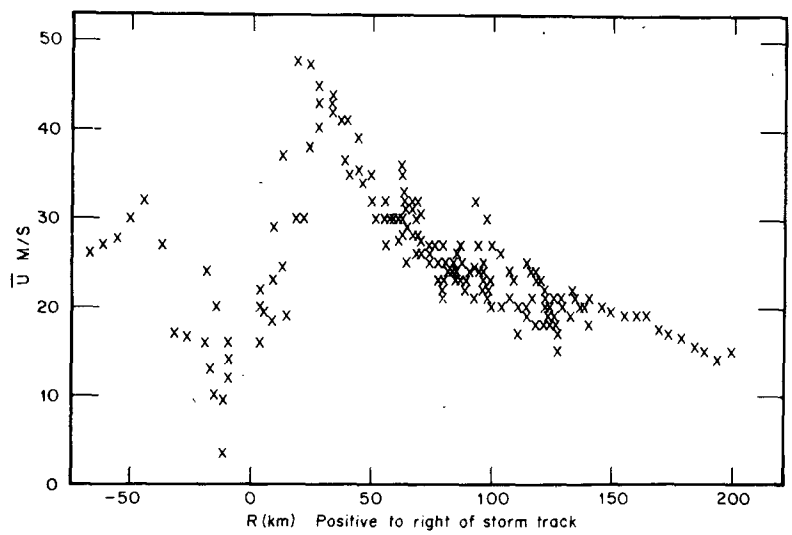

FIG. 12. Mean wind speed as a function of distance from storm center for $Z=400\pm100$ m.

5. The probability structure of the subcloud layer

The intensity of turbulent energy dissipation (ϵ) was computed from running averages of eight inertial subrange spectra by the formula

$$\epsilon = [2.2k^{5/3}E(k)]^{3/2}, \tag{3}$$

where $k = 2\pi f/\bar{U}$ is the wavenumber (m^{-1}) corresponding to frequency f (Hz) at true airspeed $\bar{U}$ (m s^{-1}) using 0.45 for Kolmogorov's constant based on Boston and Burling (1972). The distribution is approximately log-normal in the subcloud region. That is, the cumulative probability distribution for $x = \ln\epsilon$ is given by a relation close to

$$P(x) = (\sigma\sqrt{2\pi})^{-1} \exp[-(x-\mu)^2/2\sigma^2], \tag{4}$$

where μ and σ are respectively the means and standard deviations of x. Data obeying (4) plot as a straight line on "probability paper." A typical probability plot of subcloud data is presented in Fig. 14.

The values obtained for μ vary widely, corresponding to dissipation rates ranging from 0.1 to less than 10^{-5} m^2 s^{-3}. The values of σ are much more closely bounded. The smallest σ obtained was about 2 dB and the largest was less than 7 dB. The values seemed uncorrelated with position, altitude or environment. The significance of the magnitude and variation of σ is discussed next.

Aside from whatever light these observations may shed on the continuing controversy about the log-normality of ϵ (see, e.g., Kolmogorov, 1962; Van Atta and Yeh, 1975), a topic which is beyond the scope of this paper, they have an important consequence for the estimation of mean values of ϵ from the spectral data. Because of the large dynamic range involved (>30 dB) the data processing devices we use work with $\log\epsilon$ rather than with ϵ. When we compute mean values of ϵ, we actually compute the mean (μ_{10}) of $\log_{10}\epsilon$ and then define a weighted mean ϵ as

$$\hat{\epsilon} \equiv 10^{\mu_{10}}.$$

This value does not equal the true mean $\bar{\epsilon}$ given by averaging ϵ itself. Nonetheless, we can compute the true mean if we know $P(x)$ from

$$\bar{\epsilon} = \int_{-\infty}^{\infty} e^x P(x)dx.$$

Given that $P(x)$ obeys Eq. (4), we may perform the integration to obtain

$$\bar{\epsilon}/\hat{\epsilon} = \exp(\sigma^2/2). \tag{5}$$

The relation (5) is presented in Fig. 15 for σ measured in decibels. For $2 \leqslant \sigma \leqslant 7$ dB, ϵ underestimates $\bar{\epsilon}$ by a factor ranging from 1.1 to 3.6. Because of the labor involved in computing $P(x)$, the values of ϵ presented throughout this paper are values of $\hat{\epsilon}$ unless otherwise indicated.

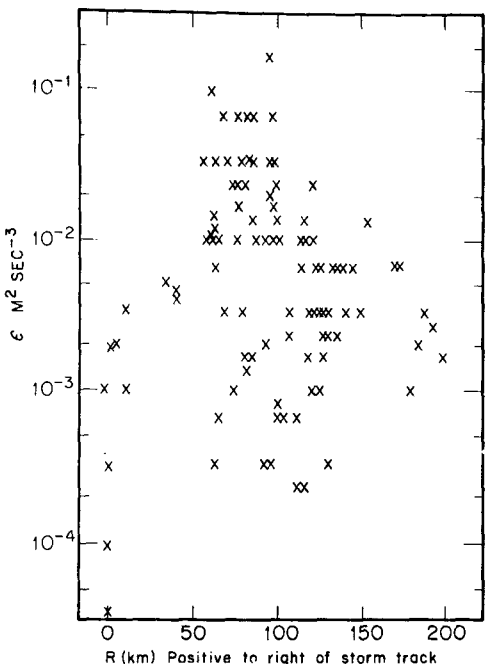

FIG. 13. Intensity of turbulent energy dissipation ϵ as a function of distance from storm center for $Z = 400 \pm 100$ m.

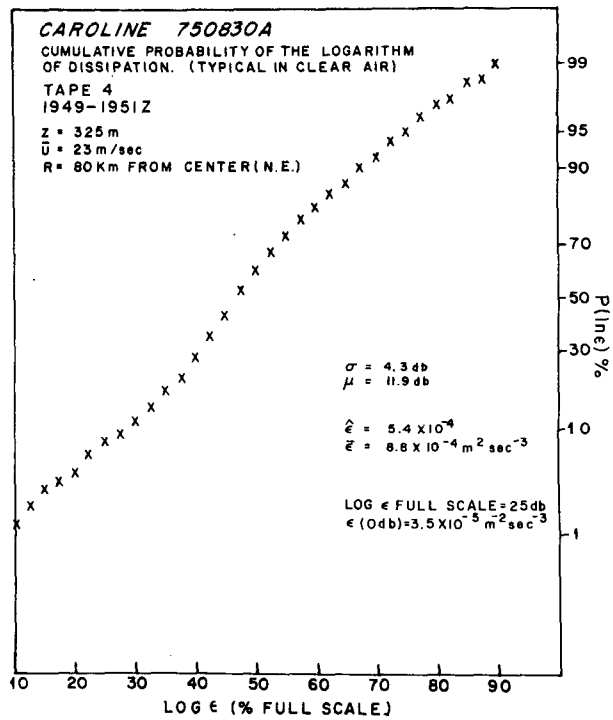

FIG. 14. Typical subcloud probability distribution of log ϵ.

6. Variation of turbulence properties with altitude

Within the boundary layer (essentially, below cloud base), the characteristics of the turbulence are uniform.

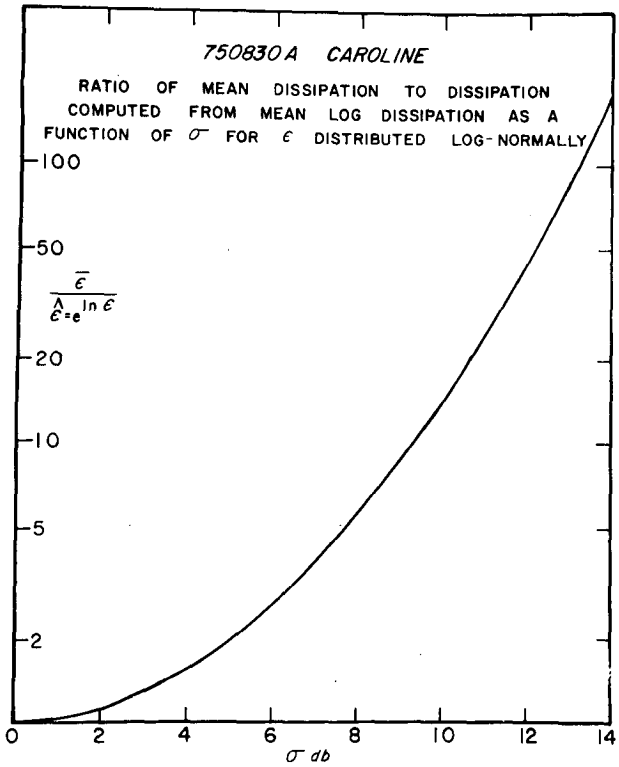

FIG. 15. Ratio of $\bar{\epsilon}$ to $\hat{\epsilon}$ for various values of σ if the probability distribution of ϵ is a log-normal.

The spectra are straight lines on a log-log presentation and their slope indicates nearly inertial subrange conditions over the scales considered here. As the top of the subcloud layer is reached, conditions begin to change. The spectra begin to show a change of shape at the higher frequencies and are no longer straight. At still higher altitudes the spectra are humped, with large peaks at scales of 10 to 20 cm. Their shape at the higher frequencies is remarkably like that of oceanic turbulence influenced by buoyancy (Belyaev *et al.*, 1975, Fig. 8) but the scales involved here are too small for simple buoyancy effects. Even at the higher altitudes, the spectra remain inertial over scales from 10 m to about 50 cm. The variation of spectral shape with altitude is shown in Fig. 16. The small-scale structure at higher altitudes is surprising and remains to be explained.

The turbulence intensities measured by the dissipation rate computed from the initial portions of the spectra show no systematic variation with height. The sample size is small, but turbulence at the higher levels seems to be as energetic as that below, at least in the region of active convection in which our higher altitude data were taken.

Because the higher altitude data were valid only in short segments, we were unable to compute probability distributions above 1000 m. Below 1000 m all of the distributions were log-normal or nearly so, even when non-inertial effects were obvious in the spectra. This confirms the results obtained in buoyancy-dominated regions sampled during the GATE (Merceret, 1976b) and probably is valid in the flow above as well.

7. Energy dissipation and the energy budget

Bulk energy budget studies of 1958 hurricanes Daisy (Riehl and Malkus, 1961) and Helene (Miller, 1962) led to the conclusion that within a cylinder of 60 n mi radius centered on each storm, internal dissipation averaged about 5×10^{14} kJ day^{-1} compared to only about 2×10^{14} kJ day^{-1} for surface layer dissipation. The matter can now be examined directly rather than through the computation of residuals used in the previous studies. The preliminary analysis confirms the results of the budget studies.

Consider a cylindrical column 60 n mi in radius and 10 km deep having a mean density of 0.8 kg m^{-3}. Let this volume be occupied by a storm having a mean dissipation rate $\bar{\epsilon}$ of 8×10^{-3} m^2 s^{-3} over 90% of its volume and 8×10^{-2} m^2 s^{-3} over the remaining 10% with a mean wind speed profile approximating that shown in Fig. 12. The volume selected is slightly smaller than that used by the authors cited above because it does not extend to the top of the atmosphere, but the dissipation above 10 km may be neglected for our purposes here. The mean dissipation rates ($\bar{\epsilon}$, not $\hat{\epsilon}$) and their percentage weightings are based on the data presented in this paper. The formula of Miller (1962) is used for surface layer dissipation. The resulting internal dissipation is 4.3×10^{14} kJ day^{-1} and the

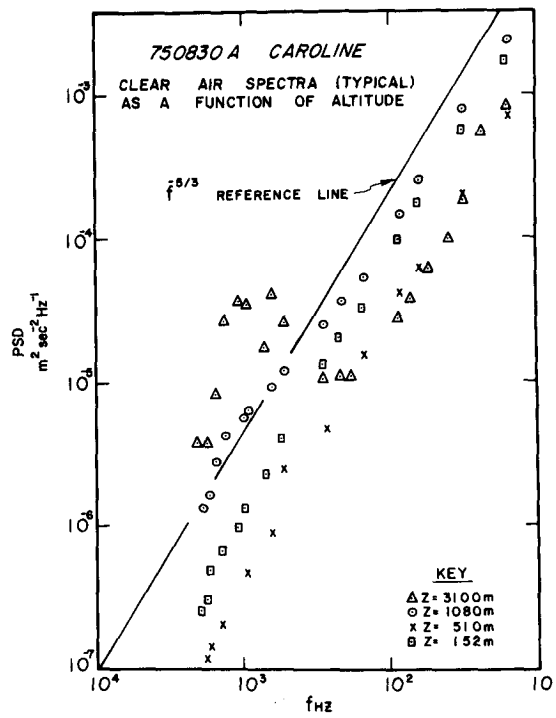

FIG. 16. Variation of spectral shape with altitude. Spectra are averages of 512 individual spectra from 0.125 s records.

surface layer dissipation is at most 2.8×10^{14} kJ day^{-1}. The errors involved in both the previous analyses and the ones here are large enough so that the close numerical agreement may be considered fortuitous. The calculations and the measurements confirm, however, that internal dissipation is of the same order as, and probably slightly larger than, the surface layer dissipation. Clearly, the internal dissipation cannot be neglected in analytical and numerical modeling of hurricanes if the physics of the systems is to be accurately represented.

8. Conclusion

While not a detailed analysis of the turbulent microstructure of hurricanes, these preliminary results from Caroline establish certain experimental findings:

1) Below cloud base, the horizontal velocity field at small scales is inertial and the dissipation log-normally distributed.

2) Above cloud base, the finestructure is altered but the dissipation rate does not appear to change significantly.

3) The dependence of ϵ on wind speed outside of the eye is too small to be detected above the background of its stochastic variation, at least for wind speeds up to 30 m s^{-1}. A small sample at altitudes up to 3000 m indicates no significant variation with height.

4) As predicted from bulk budget studies of previous storms, the energy dissipated internally above the surface layer is larger than that dissipated near the surface by roughly a factor of two.

These findings establish for the first time a direct observational foundation for dealing with the energetics and distribution of turbulence in tropical storms.

Acknowledgments. The author thanks the Research Facilities Center (NOAA), the Boundary Layer Dynamics Group (ERL, NOAA) and the Hurricane and Support groups of NHEML (NOAA) for their assistance in the conduct and publication of this research, and the National Environmental Satellite Service (NOAA) for the SMS-1 photograph of Fig. 5. The use of the wind tunnel at the School of Engineering of the University of Miami for calibration of the instruments is gratefully acknowledged.

REFERENCES

Belyaev, V. S., A. N. Gezentsvey, A. S. Monin, R. V. Ozmidov and V. T. Paka 1975: Spectral characteristics of small-scale fluctuations of hydrophysical fields in the upper layer of the ocean. *J. Phys. Oceanogr.*, **5**, 492–498.

Boston, N. E. J., and R. W. Burling 1972: An investigation of high-wavenumber temperature and velocity spectra in air. *J. Fluid Mech.*, **55**, 473–492.

Jenkins, G. M., and D. G. Watts 1968: *Spectral Analysis and Its Applications.* Holden-Day, 525 pp.

Kolmogorov, A. N., 1962: A refinement of previous hypotheses concerning the local structure of turbulence in a viscous incompressible fluid at high Reynolds number. *J. Fluid Mech.*, **13**, 82–85.

Merceret, F. J., 1976a: Measuring atmospheric turbulence with airborne hot-film anemometers. *J. Appl. Meteor.*, **15**, 482–490.

——, 1976b: Airborne hot-film measurements of the small scale structure of atmospheric turbulence during the GATE. *J. Atmos. Sci.*, **33** (in press).

Miller, B. I., 1962: On the momentum and energy balance of hurricane Helene 1958. NHRP Rep. No. 53, U. S. Dept. of Commerce, NOAA, Coral Gables, Fla., 19 pp.

Pennell, W. T., and M. A. Lemone, 1974: An experimental study of turbulence structure in the fair-weather trade wind boundary layer. *J. Atmos. Sci.*, **31**, 1308–1323.

Riehl, H., and J. Malkus, 1961: Some aspects of hurricane Daisy 1958. NHRP Rep. No. 46, U. S. Dept. of Commerce, NOAA, Coral Gables, Fla., 64 pp.

Van Atta, C. W., and T. T. Yeh, 1975: Evidence for scale similarity of internal intermittency in turbulent flows at large Reynolds numbers. *J. Fluid Mech.*, **71**, 417–440.